

Regular article

A theoretical investigation of (–)-deprenyl (selegiline) as a radical scavenger

Sachiko Nakai, Fumio Yoneda

Fujimoto Pharmaceutical Corporation, 1-3-40 Nishi-Otsuka, Matsubara-shi, Osaka 580-8503, Japan

Received: 6 October 1999 / Accepted: 5 March 2000 / Published online: 21 June 2000
© Springer-Verlag 2000

Abstract. The chemical reactions between (–)-deprenyl and $\cdot\text{OH}$ or $\cdot\text{OOH}$ were studied using molecular orbital theory, with *N,N*-dimethylpropargylamine as a model. (–)-Deprenyl was confirmed to be a good radical scavenger. The active site was the acetylenic part and $\cdot\text{OH}$ - or $\cdot\text{OOH}$ was trapped on either acetylenic carbon. The activation energies were about 10–20 kcal/mol. The resulting $\cdot\text{OH}$ - or $\cdot\text{OOH}$ -adducts, still radicals, trapped further radicals on the remaining carbon of the acetylenic part. The final double trapping products were at extraordinarily lower energy levels than the original reactants by 50–70 kcal/mol. The secondary transition states were not detected, suggesting that the reactions occurred at once or in a cascade. Some results with the model system were verified by the results with the real (–)-deprenyl system.

Key words: (–)-Deprenyl – Oxidative stress – $\cdot\text{OH}$ – $\cdot\text{OOH}$ – Radical scavenger

1 Introduction

(–)-Deprenyl [1] (selegiline) is a selective irreversible inhibitor of type B monoamine oxidase (MAO-B) [2] and has been widely used in the clinical treatment of Parkinson's disease in combination with levodopa as a dopamine precursor [3]. Parkinson's disease is a neurodegenerative disorder characterized by the deficiency of dopamine as a chemical transmitter due to degeneration of dopaminergic neurons in the nigrostriatal pathway [4]. Its symptoms are ameliorated by dopaminergic therapy based on treatment with levodopa. (–)-Deprenyl has ability to potentiate and prolong the efficacy of levodopa, since (–)-deprenyl inhibits the oxidative catabolism of dopamine by MAO-B. The inhibition mechanism of MAO-B by (–)-deprenyl has been investigated extensively from chemical, biological and theoretical points of view [5].

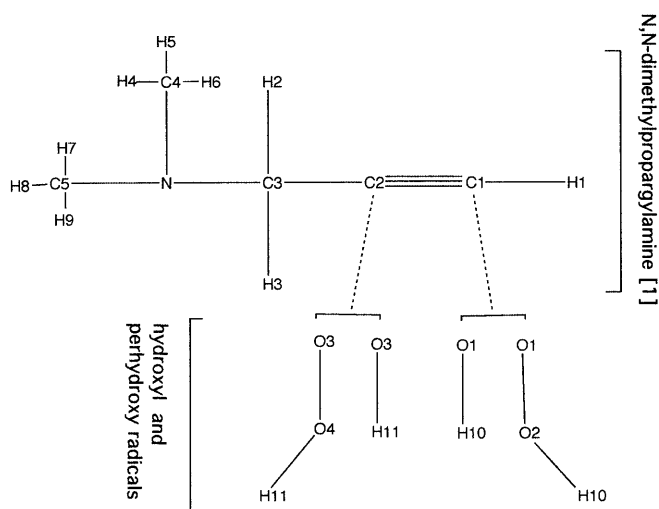
In the meantime, evidence has been presented which suggests that (–)-deprenyl may protect the central nervous system (CNS) from oxidative insults by virtue of radical scavenging activities [6]. For example, Wu et al. [7] have demonstrated that (–)-deprenyl can suppress the generation of the cytotoxic hydroxyl radical ($\cdot\text{OH}$) and hence can contribute to the preservation of nigral neurons from possible oxidative stress caused by 1-methyl-4-pyridinium.

(–)-Deprenyl also inhibits the nonenzymatic autoxidation of dopamine, which is known to lead to the generation of $\cdot\text{OH}$ and a semiquinon radical and to the formation of melanin pigment [8]. Recently, Thomas et al. [9] have demonstrated that (–)-deprenyl is also a potent inhibitor of secondary radicals such as the lipid-derived perhydroxy radical ($\cdot\text{OOH}$). These facts emphasize that (–)-deprenyl appears to have some remarkable neuroprotective properties besides the role of a MAO-B inhibitor.

The present article describes a quantum chemical investigation of the reactions between (–)-deprenyl and $\cdot\text{OH}$ or $\cdot\text{OOH}$. We used a simplified model of (–)-deprenyl, *N,N*-dimethylpropargylamine (**1**) shown in Fig. 1, in order to follow the reactions in detail. Some of the reaction products were calculated using (–)-deprenyl itself for verification of the results.

2 Method

The geometry optimizations were calculated by ab initio molecular orbital theory using the Gaussian94 program [10]. The results presented here are mainly based on method A that is designated for Hartree–Fock (HF) self-consistent-field theory at the 6-31G(d) level. Some systems were calculated by method B, which is designated for second-order Møller–Plesset perturbation theory [11] (MP2) at the 6-31G(d) level, in order to confirm the results obtained by method A. The calculations for the systems containing (–)-deprenyl itself were done at the HF/3-21G level. The restricted HF method was used for closed-shell systems and the unrestricted HF (UHF) method was used for radical open-shell systems. The atomic charges were calculated by Mulliken population



(-)-deprenyl

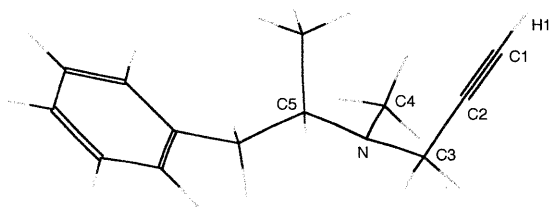


Fig. 1. The reaction systems and notations. (-)-Deprenyl is also shown

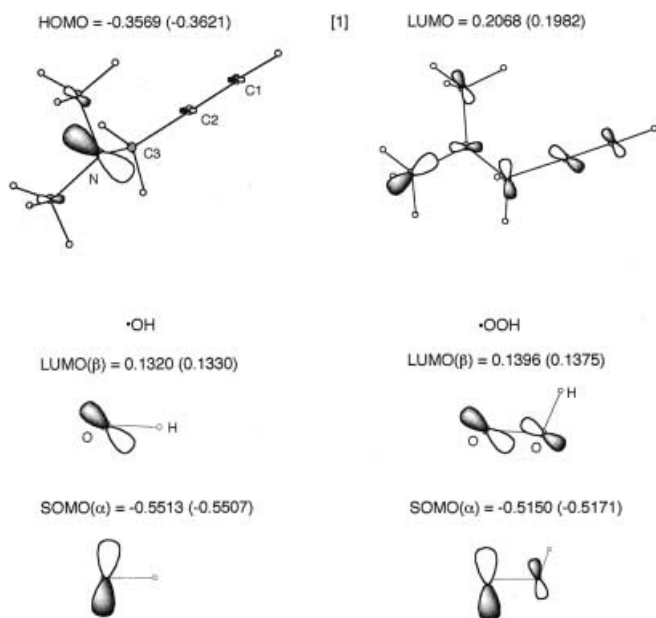


Fig. 2. The frontier molecular orbitals of the reactants obtained by method A. The values are in atomic units; the values in parentheses were obtained by method B

analysis. The frequency analyses for verification of the transition states were computed through the second derivatives of the energy with respect to the Cartesian nuclear coordinates in the Gaussian94 program.

3 Frontier molecular orbitals of the reactants

The molecular orbitals of **1** and the radicals $\cdot\text{OH}$ and $\cdot\text{OOH}$ obtained by method A are represented in Fig. 2. The energy levels of the orbitals are shown in atomic units and the values in parentheses are the results obtained by method B. It is observed that the highest occupied molecular orbital of **1** has a large lobe at the N position; however, this position did not make a bond connection with the radicals and the singly occupied molecular orbitals (SOMOs) of the radicals came into contact with the lowest unoccupied molecular orbital (LUMO) of **1** on C1 or C2 of the triple bond (vide infra). The orbitals of $\cdot\text{OH}$ and $\cdot\text{OOH}$ were very similar to each other in the terminal O position (O1 or O3 in Fig. 1).

4 $\cdot\text{OH}$ trapping

The chemical reaction processes between **1** and $\cdot\text{OH}$ are shown in Fig. 3. There are two routes for the reaction: one is the trapping of $\cdot\text{OH}$ on the C1 site of **1** and the other is the trapping on the C2 site. The reactants, **1** and $\cdot\text{OH}$, two transition states, TS2 and TS2', and two products, **2** and **2'**, are represented in the figure. The energy variations along the intrinsic reaction coordinates (IRC), which are calculated using method A, are also shown. These curves are independent of each other but are conveniently drawn on the same coordinates, taking the energy level of the reactants as the energy base line. The activation energies for TS2 and TS2' from the reactants are 11.7 and 12.8 (11.2 and 10.1) kcal/mol, respectively, where the values in parentheses are the ones obtained by method B. The products **2** and **2'** are lower in energy by 39.1 and 35.8 (44.8 and 36.9) kcal/mol than the respective transition states. This means that **2** and **2'** are more stable by 27.4 and 23.0 (33.6 and 26.8) kcal/mol than the reactants, respectively.

The bond lengths and angles are also shown in Fig. 3. The acetylenic triple bond C1—C2 of **1** was elongated as $1.187 \rightarrow 1.255 \rightarrow 1.328 \text{ \AA}$ for the reaction $\mathbf{1} + \cdot\text{OH} \rightarrow \text{TS2} \rightarrow \mathbf{2}$ and as $1.187 \rightarrow 1.245 \rightarrow 1.325 \text{ \AA}$ for the reaction $\mathbf{1} + \cdot\text{OH} \rightarrow \text{TS2}' \rightarrow \mathbf{2}'$. Also the angles of C1—C2—C3 of **1** were bent as $178.94 \rightarrow 146.59 \rightarrow 123.99^\circ$ for the process toward **2** and as $178.94 \rightarrow 157.84 \rightarrow 136.25^\circ$ for the process toward **2'**. The other parts of the molecules were not changed much. Similar trends were found for the results obtained by method B, cf. the corresponding values in parentheses in the figure.

Consequently, it is concluded that the two reactions, $\mathbf{1} + \cdot\text{OH} \rightarrow \text{TS2} \rightarrow \mathbf{2}$ and $\mathbf{1} + \cdot\text{OH} \rightarrow \text{TS2}' \rightarrow \mathbf{2}'$, are quite similar to each other, energetically and geometrically, and will proceed very easily; $\cdot\text{OH}$ is trapped on either C1 or C2 unselectively.

5 $\cdot\text{OOH}$ trapping

As **1** reacts with $\cdot\text{OH}$, it is also expected to react with $\cdot\text{OOH}$ because their molecular orbitals are very similar (Fig. 2). The reactions between **1** and $\cdot\text{OOH}$ are shown in Fig. 4. There are two routes for the trapping of $\cdot\text{OOH}$

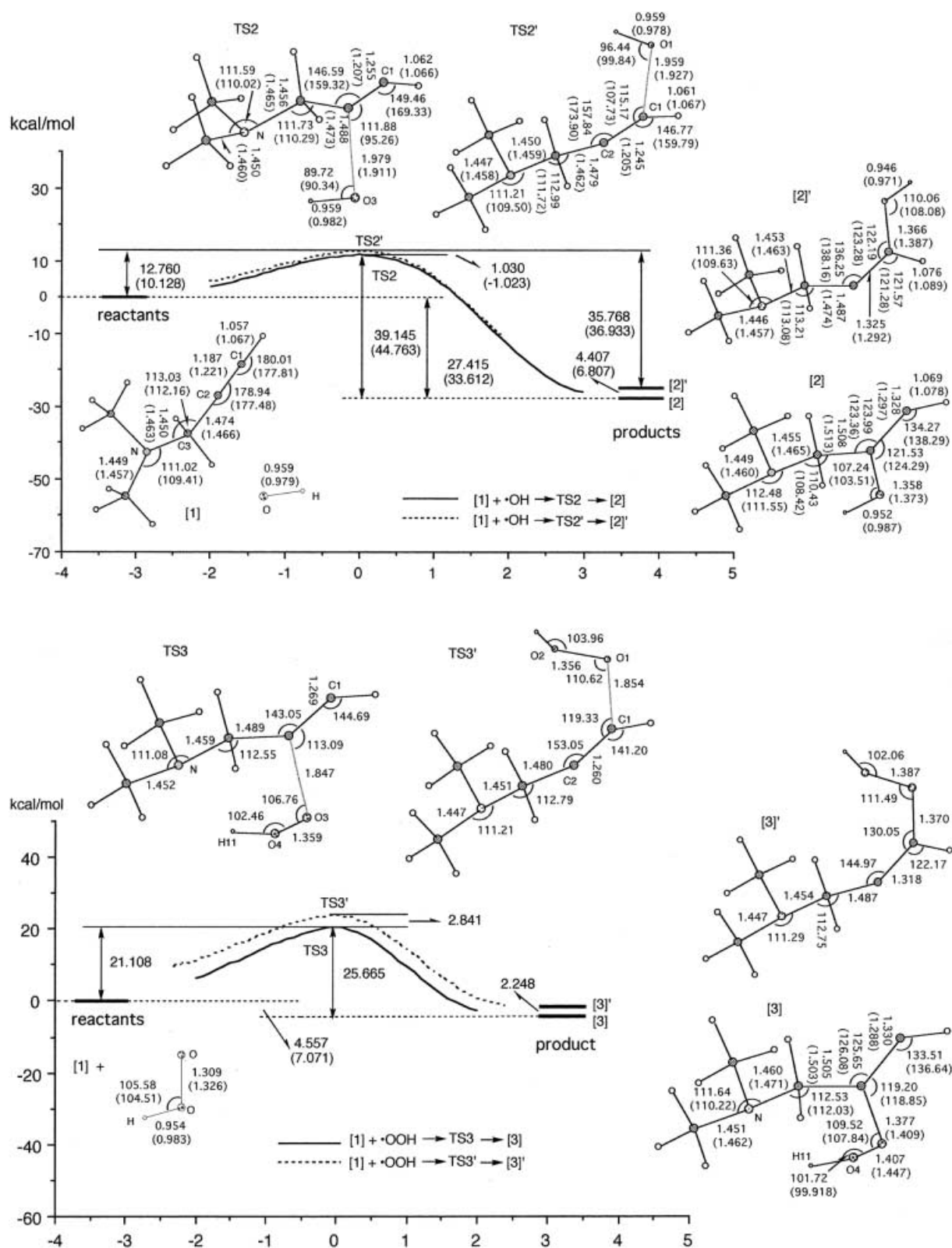


Fig. 4. Two reaction processes of $\cdot\text{OOH}$ trapping. See the caption to Fig. 3

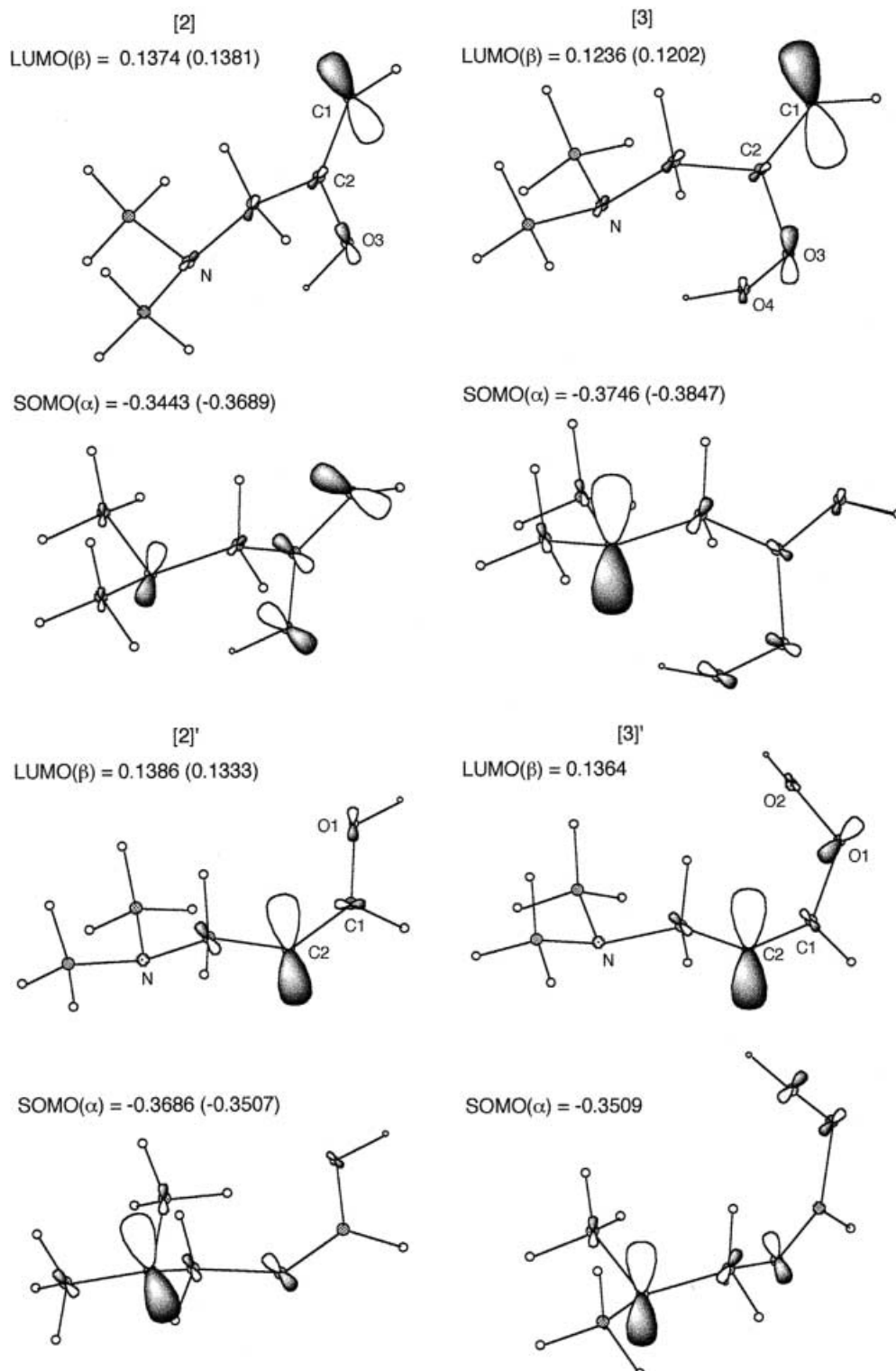
as in the case of $\cdot\text{OH}$; one is the trapping on C1 and the other is the trapping on C2 of **1**. Two transition states, TS3 and TS3', and two products, **3** and **3'**, are represented in the figure. The energy variations along

the IRC are also shown, where the energy level of the reactants, **1** and $\cdot\text{OOH}$, was taken as the base line. The activation energies for TS3 and TS3' were 21.1 and 23.9 kcal/mol, respectively, which were larger than those

◀
Fig. 3. Two reaction processes of $\cdot\text{OH}$ trapping. The energy curves are independent of each other but are plotted on the same intrinsic reaction coordinates ($\text{amu}^{-1/2} \text{ bohr}$). The *numbers* in the configurations of the molecules are in angstroms for the lengths and in degrees for the angles. The energies are in kilocalories per mole and the *numbers in parentheses* were obtained by method B and are not scaled

in the $\cdot\text{OH}$ trapping. The energy levels of the products **3** and **3'** were lower than those of the reactants by only 4.6 and 2.3 kcal/mol, respectively. The characteristic bond lengths and angles of every state are shown in the figure. The conformational changes along the reaction processes are observed to be very similar to those of the $\cdot\text{OH}$ trap-

Fig. 5. The frontier orbitals of the primary radical trapping products. The values are in atomic units; the values in *parentheses* were obtained by method B



ping. The bond length C1—C2 changes as 1.187 \rightarrow 1.269 \rightarrow 1.330 Å for the reaction $\mathbf{1} + \cdot\text{OOH} \rightarrow \text{TS3} \rightarrow \mathbf{3}$ and as 1.187 \rightarrow 1.260 \rightarrow 1.318 Å for the reaction $\mathbf{1} + \cdot\text{OOH} \rightarrow \text{TS3}' \rightarrow \mathbf{3}'$. The bond angle C1—C2—C3 changes as 178.94 \rightarrow 143.05 \rightarrow 125.65° toward the product $\mathbf{3}$ and as 178.94 \rightarrow 153.05 \rightarrow 144.97° toward the product $\mathbf{3}'$. The other parts were not changed much, similarly to the $\cdot\text{OH}$ trapping case.

These reactions were only calculated by method A, except for the product $\mathbf{3}$, for which the results obtained by method B were similar to those obtained by method A as seen from the values in parentheses. Thus, it has been found that the $\cdot\text{OOH}$ trapping by $\mathbf{1}$ needed more activation energy and gave less stable products than in the reactions of $\cdot\text{OH}$ trapping.

6 Secondary reactions

Since the products $\mathbf{2}$ or $\mathbf{2}'$, and $\mathbf{3}$ or $\mathbf{3}'$ are still in radical states, they can react with further $\cdot\text{OH}$ or $\cdot\text{OOH}$. The molecular orbitals of these radical products calculated by method A are shown in Fig. 5. The LUMOs have large lobes on C1 for $\mathbf{2}$ and $\mathbf{3}$ and on C2 for $\mathbf{2}'$ and $\mathbf{3}'$. On the other hand, the SOMOs have quite small lobes on these sites, except that for $\mathbf{2}$. It is considered that as in the primary reactions the large lobes of the SOMOs on N are for electron-donating not for bond-making with radicals. Thus the large lobes of the LUMOs on C1 or C2 are considered to serve for the secondary trapping of $\cdot\text{OH}$ or $\cdot\text{OOH}$ and additionally the small lobes of the SOMOs on these sites could be involved somewhat in the trapping.

As a consequence of the double trappings on C1 and C2, the singlet state products $\mathbf{4}$ and $\mathbf{5}$ were found. If both $\cdot\text{OH}$ and $\cdot\text{OOH}$ are present in the surroundings, mixed trapping products such as $\mathbf{6}$ or $\mathbf{7}$ would be obtained. The conformations and energy levels of these secondary products are shown in Fig. 6. The configurational changes from $\mathbf{1}$ are localized around the acetylenic part and the rest are almost unchanged. The

transition states for the secondary reactions could not be found. These radical–radical reactions could occur at once or in a cascade without passing into the transition states. Thus, the energy levels of the secondary products were lower by 50–80 kcal/mol than those of the original reactants and consequently it could be proved that $\mathbf{1}$ is a good radical scavenger. The calculations of these products of the secondary reactions, which are all in singlet states, were done by method A alone.

7 Charge variations along the reactions

Table 1 presents the spin densities of the radical products and transition states, listing only the values for the atoms which have spins. The spins on the other atoms were zero or nearly zero. The upper lines show the results obtained by method A and the second lines those obtained by method B. It is observed that the spins, which were on O of $\cdot\text{OH}$ or mainly terminal O of $\cdot\text{OOH}$ at the beginning of the reactions, were transferred to the untouched carbon C1 or C2 of the products at the end, passing the transition state where the electron was distributed both on C1 and on C2. At the bottom of Table 1, the S^2 values for each radical state are given. It is observed that, the spin contaminations are quite large in the results for the transition states obtained by method A but these are ameliorated in the results obtained by method B.

The charge densities on the atoms along the processes are presented in Table 2. The densities on the other atoms scarcely changed. In TS2 and TS3, in $\mathbf{2}$ and $\mathbf{3}$, in TS2' and TS3', in $\mathbf{2}'$ and $\mathbf{3}'$, and in $\mathbf{4}$, $\mathbf{5}$, $\mathbf{6}$ and $\mathbf{7}$, the charge distributions were similar to each other, respectively. It is remarkable that in contact with radicals, the charges on C1 of $\mathbf{1}$ become almost zero and the

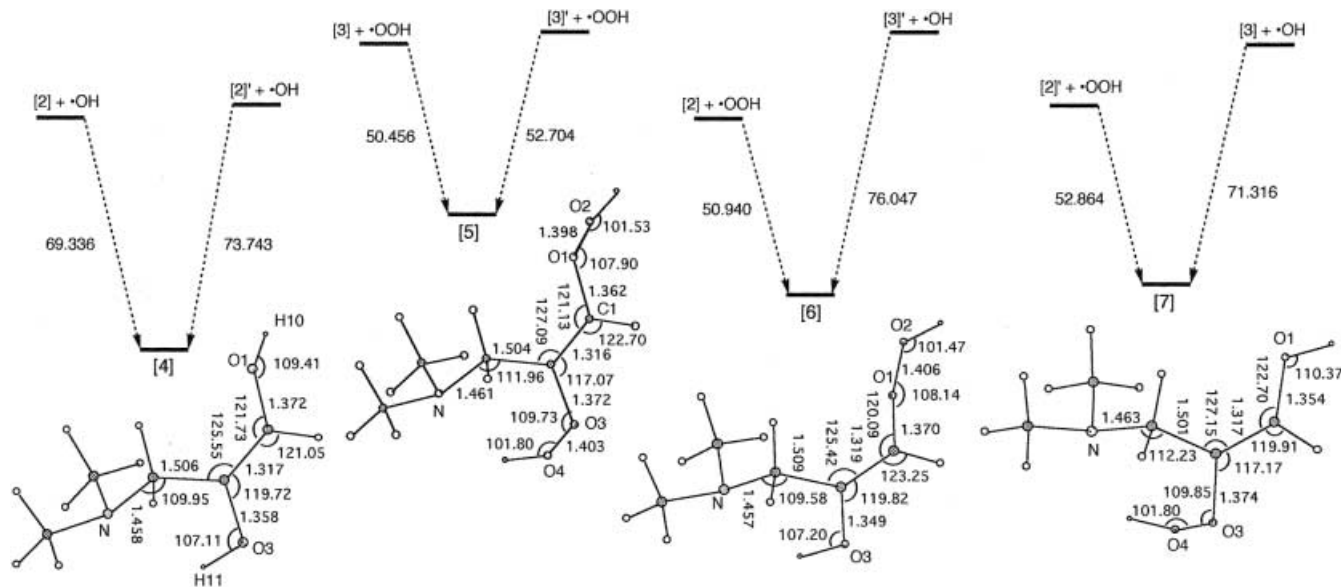


Fig. 6. The double radical trapping products and the energy diagrams. The numbers in the configurational pictures are in angstroms for the lengths and in degrees for the angles. The energies are in kilocalories per mole

Table 1. The spin densities and S^2 values. The *first lines* were obtained by method A, the *second lines* by method B for the model system and the *third lines* by the UHF/3-21G method for the real (-)-deprenyl system. The values in the *left-most column* of the

reactants are compared with the corresponding lines of the products. **1** has no spin density. The S^2 values of the reactants $\cdot\text{OH}$ and $\cdot\text{OOH}$ were all 0.750

Reactants		Atom	TS2	2	TS3	3	TS2'	2'	TS3'	3'
1	–	C1	1.426	1.670	1.499	1.719	–1.107	–0.673	–1.141	–0.630
			1.134	1.585		1.606	–0.855	–0.599		
	–	C2	–1.240	–0.677	–1.230	–0.761	1.303	1.637	1.413	1.590
			–0.909	–0.609		–0.664	1.048	1.543		
	–	C3	0.125	0.079	0.122	0.085	–0.144	–0.133	–0.147	–0.145
	0.100		0.045	0.076		–0.126	–0.131			
–	H1	–0.076	–0.058	–0.073	–0.062	0.068	0.058	0.068	0.062	
		–0.074	–0.055		–0.057	0.060	0.058			
$\cdot\text{OH}$		O1	–	–	–	–	0.844	0.017	0.739	0.041
			0.847	0.030	–0.008	–0.006				
O	1.051	O2	–	–	–	–	–	–	–	–
	1.054		–	–	–	–	–	–	–	–
	1.070									
H	–0.051	H10	–	–	–	–	–0.040	0.008	–0.003	–0.001
	–0.054		–	–	–	–0.043	0.008	–	–	
	–0.067									
$\cdot\text{OOH}$		O3	0.862	0.014	0.751	0.140	–	–	–	–
	First		0.920	0.836		0.026	0.163	–	–	–
	O									
	1.134									
Second	0.091	O4	–	–	–0.008	–0.086	–	–	–	–
	O		0.074	–		–	–0.094	–	–	–
	–0.134									
H	–0.011	H11	–0.035	0.006	–0.002	0.002	–	–	–	–
	–0.011		–0.037	0.005		0.002	–	–	–	–
	0.000									
		S^2	0.894	0.756	0.907	0.762	0.837	0.756	0.864	0.756
			0.783	0.754		0.758	0.774	0.754		
			0.929	0.757						

charges on C2 become more positive, losing electrons. On the radical sides, the oxygens gain more electrons by being trapped, i.e. the opposite to the movement of the spins.

8 Results with the real (-)-deprenyl system

The study described previously was pursued using a simplified model system. It is necessary to check if the reactions with real (-)-deprenyl system proceed as with the model system, i.e. to check whether or not the other parts of (-)-deprenyl except for the model part interfere in the reaction in question. The products **2a**, **4a** and **6a**, were found by calculations at the (U)HF/3-21G level, which correspond to **2**, **4** and **6**, respectively. The results are represented in Fig. 7. The energy differences of **2a**, **4a** and **6a** from the respective reactants were in good agreement with the results already mentioned. The spin densities and the atomic charge densities of these real

systems were observed to show the same tendency as in the model system, of which the values of the corresponding atoms are presented in the third lines in Tables 1 and 2.

Furthermore the possibility of $\cdot\text{OH}$ additions on the phenyl group of (-)-deprenyl was examined and compared with the ones on the acetylenic part. Thus the products **8a**, **9a** and **10a** were found as shown in Fig. 7. The product **8a** is the adduct of $\cdot\text{OH}$ on the para position of the phenyl group. The activation energy for **8a** was 8.5 kcal/mol, which was almost the same as that for **2a** (8.7 kcal/mol); however the energy level of **8a** was 18.0 kcal/mol higher than that of **2a**. The $\cdot\text{OH}$ adduct on the ortho position (omitted in the figure) was also found at almost the same energy level as **8a**. The product **9a** is an adduct of two $\cdot\text{OH}$ s on the phenyl group and the energy level of **9a** is higher by 52.2 kcal/mol than that of **4a**. The product **10a** is also an adduct of two $\cdot\text{OH}$ s, one on the phenyl group and the other on the acetylenic carbon. This product is obtained only in the triplet state,

Table 2. The atomic charge densities. See the caption to Table 1

Reactants	Atom	TS2	2	TS3	3	TS2'	2'	TS3'	3'	4	5	6	7	
1		-0.519	-0.295	-0.295	-0.270	-0.238	-0.272	0.076	-0.198	0.089	0.018	0.136	0.061	0.093
		-0.473	-0.306	-0.308		-0.252	-0.347	0.078						
		-0.442		-0.208							0.055		0.082	
		0.163	0.099	0.378	0.135	0.367	0.109	-0.010	0.088	0.006	0.363	0.334	0.377	0.318
		0.124	0.096	0.395		0.376	0.170	0.005						
		-0.005		0.258							0.313		0.348	
		-0.144	-0.155	-0.181	-0.142	-0.159	-0.182	-0.169	-0.189	-0.173	-0.178	-0.163	-0.182	-0.160
		-0.164	-0.151	-0.187		-0.162	-0.174	-0.179						
		-0.205		-0.242							-0.230		-0.240	
		-0.541	-0.588	-0.602	-0.601	-0.605	-0.543	-0.546	-0.546	-0.543	-0.605	-0.609	-0.611	-0.605
		-0.533	-0.576	-0.613		-0.626	-0.528	-0.537						
		-0.691		-0.728							-0.733		-0.737	
		0.285	0.244	0.203	0.242	0.220	0.241	0.181	0.234	0.210	0.187	0.223	0.192	0.211
	0.291	0.269	0.208		0.226	0.255	0.180							
	0.332		0.240							0.235		0.245		
						-0.549	-0.711	-0.198	-0.359	-0.771	-0.406	-0.384	-0.714	
	O1	-	-	-	-	-0.552	-0.720							
										-0.701		-0.418		
·OH														
O		-0.444						-0.423	-0.433		-0.463	-0.452		
		-0.442												
		-0.370										-0.408		
H		0.444				0.436	0.454	0.458	0.466	0.449	0.467	0.458	0.464	
		0.442				0.432	0.452							
		0.370								0.386		0.406		
·OOH														
First		-0.076	-0.574	-0.755	-0.208	-0.391	-	-	-	-0.731	-0.381	-0.763	-0.407	
O		-0.069	-0.581	-0.774	-0.402									
		-0.026		-0.722						-0.748		-0.746		
Second		-0.391		-0.449	-0.462						-0.435		-0.471	
O		-0.400			-0.484									
		-0.393												
H		0.468	0.470	0.477	0.488	0.487				0.477	0.488	0.483	0.485	
		0.468	0.459	0.487		0.508								
		0.419		0.417						0.420		0.428		

which means that the additions of ·OH on the phenyl group and on the acetylenic carbon seem to be independent of each other, making radical states in separate parts of the molecule. The energy level of **10a** was higher than that of **4a** by 61.8 kcal/mol. Consequently, these results indicated that the most stable product was **4a** obtained by the double trapping of ·OHs on the acetylenic part. Some characteristic bond lengths of each product are shown in Fig. 7. They show that the configurational changes are very localized. The ·OOH addition on the phenyl group occurred in the same way as the ·OH addition described previously; however, the addition of the para position, corresponding to **8a**, needed an activation energy of 19.0 kcal/mol and the energy level of the adduct was higher by 11.2 kcal/mol than that of the reactants. Namely, the ·OOH trappings on the phenyl group were harder than the corresponding ·OH trappings.

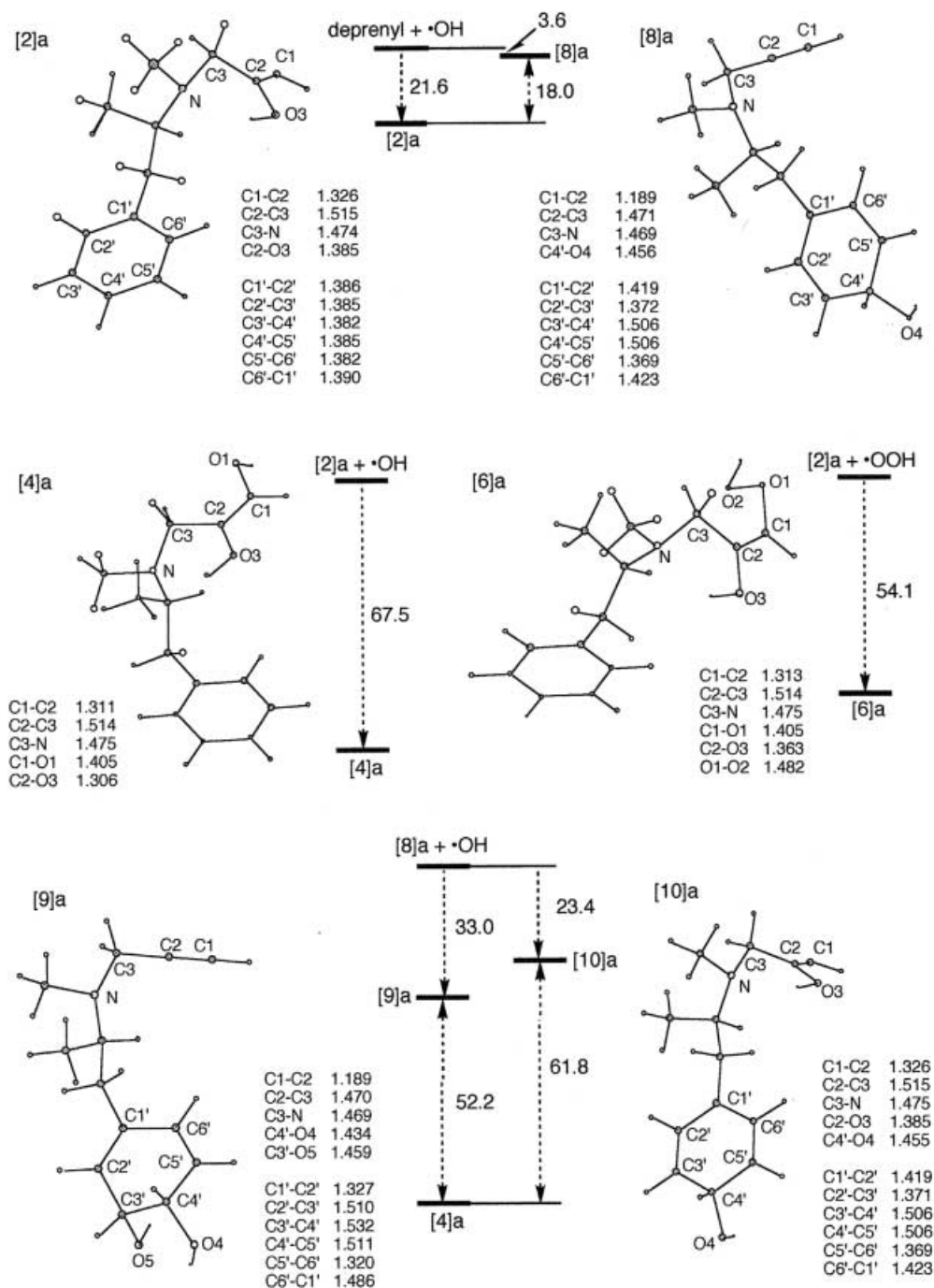
Thus, it was confirmed that our studies using the model without the phenyl ring represent well the radical scavenging functions of the real (-)-deprenyl system.

9 Discussion and conclusion

The results obtained through method A gave fine and reasonable features for the reactions of **1** with ·OH or ·OOH. The HF/3-21G level calculations for the real (-)-deprenyl system verified the results obtained by method A for the model system. Besides, the calculations revealed that the radical scavengings of ·OH and ·OOH on the phenyl group are possible, the chemical reactions of which proceed without interference in the reactions on the acetylenic part regarded as the main reactive center of the molecule. The phenyl group of (-)-deprenyl seems to contribute to the advantage from bioavailable and pharmacokinetic points of view. This could be supported by the recent report by Boulton [12] that *N,N*-dialkylpropargylamine possessing no phenyl group showed similar neuroprotective activity as well as MAO-B inhibition to (-)-deprenyl.

Supplementary studies through method B of higher accuracy for the reactions in the open-shell systems

Fig. 7. The radical trapping products in the real (-)-deprenyl system. The energy diagrams (kcal/mol) and some characteristic bond lengths (Å) are shown



$1 + \cdot\text{OH} \rightarrow \text{TS2} \rightarrow 2$ and $1 + \cdot\text{OH} \rightarrow \text{TS2}' \rightarrow 2'$ have justified the results obtained by method A.

We have established theoretically the scavenging mechanism of $\cdot\text{OH}$ and $\cdot\text{OOH}$ by (-)-deprenyl. Using *N,N*-dimethylpropargylamine as a simplified model of (-)-deprenyl, the two-step trappings of these radicals were found. The first single radical trapping on either carbon of the acetylenic part provoked the resulting products into trapping further radicals on the remaining carbon. As a consequence, the double radical trapping products were much lower in energy than the primary radical products or the

original reactants. Thus, it was concluded that (-)-deprenyl is a good and effective scavenger of $\cdot\text{OH}$ or $\cdot\text{OOH}$.

The theoretical results suggest that (-)-deprenyl might be useful as a neuroprotective drug for neurodegenerative diseases concerned with possible oxidative damages in the CNS, such as Parkinson's disease, senile dementia and Alzheimer's disease, scavenging the causative radical species such as $\cdot\text{OH}$ or $\cdot\text{OOH}$. Furthermore it may be noted that the present study analyzed theoretically the reaction mechanism of a radical addition to an acetylenic bond.

References

1. Simon K, Podányi B, Ecsery ZJ (1986) *J Chem Soc Perkin Trans II*: 111
2. (a) Bach AW, Lan NC, Johnson DL, Abell CW, Bembenek ME, Kwan SW, Seeburg PH, Shih JC (1988) *Proc Natl Acad Sci USA* 85: 4934; (b) Grimsby J, Chen Wang L-J, Lan NC, Shih JC (1991) *Proc Natl Acad Sci USA* 88: 3637; (c) Tan AK, Ramsey RR (1993) *Biochemistry* 32: 2137
3. (a) Birkmayer B, Riederer P, Youdim MBH, Linnauer W (1975) *J Neural Transm* 36: 303; (b) Knoll J (1986) *J Neural Transm Suppl* 22: 75
4. Youdim MBH, Riederer P (1997) *Sci Am* 276: 38
5. (a) Kim JM, Bogdan MA, Mariano PS (1993) *J Am Chem Soc* 115: 10591; (b) Silverman RB (1995) *Acc Chem Res* 28: 335; (c) Nakai S, Yoneda F, Yamabe T, Fukui K (1999) *Theor Chem Acc* 102: 147
6. (a) Rinne JO, Rönttö M, Paljärvi L, Rummukainen J, Rinne UK (1991) *Neurology* 41: 859; (b) Knoll J (1993) *J Neural Transm Suppl* 40: 69; (c) Gerlach M, Youdim MBH, Riederer P (1994) *J Neural Transm Suppl* 41: 177; (d) Lange KW, Rausch W-D, Gsell W, Naumann M, Oestreicher E, Riederer P (1994) *J Neural Transm Suppl* 43: 183; (e) de la Cruz CP, Revilla E, Steffen V, Rodriguez-Gómez JA, Cano J, Machado A (1996) *Br J Pharmacol* 117: 1756; (f) Fowler JS, Volkow ND, Wang G-J, Pappas N, Logan J, MacGregor R, Alexoff D, Shea C, Schlyer D, Wolf AP, Warner D, Zezulakova I, Cilento R (1996) *Nature* 379: 733
7. Wu RM, Chiueh CC, Pert A, Murphy DL (1993) *Eur J Pharmacol* 243: 241
8. Chiueh CC, Huang S-J, Murphy DL (1994) *J Neural Transm Suppl* 41: 189, and references therein
9. Thomas CE, Huber EW, Ohlweiler DF (1997) *Free Radical Biol Med* 22: 733
10. Frisch MJ, Trucks GW, Schlegel HB, Gill PMW, Johnson BG, Robb MA, Cheeseman JR, Keith T, Petersson GA, Montgomery JA, Raghavachari K, Al-Laham MA, Zakrzewski VG, Ortiz JV, Foresman JB, Cioslowski J, Stefanov BB, Nanayakkara A, Challacombe M, Peng CY, Ayala PY, Chen W, Wong MW, Andres JL, Replogle ES, Gomperts R, Martin RL, Fox DJ, Binkley JS, Defrees DJ, Baker J, Stewart JP, Head-Gordon M, Gonzalez C, Pople JA (1995) *Gaussian 94*, revision E.3. Gaussian, Pittsburgh, Pa
11. (a) Møller C, Plesset MS (1934) *Phys Rev* 46: 618; (b) Handy C, Schaefer HF III (1984) *J Chem Phys* 81: 5031; (c) Frisch MJ, Head-Gordon M, Pople JA (1990) *Chem Phys Lett* 166: 281
12. Boulton AA (1999) *Mech Aging Dev* 111: 201